© EARSeL and Warsaw University, Warsaw 2005. *Proceedings of 4th EARSeL Workshop on Imaging Spectroscopy. New quality in environmental studies*. Zagajewski B., Sobczak M., Wrzesień M., (eds)

EVALUATION OF ENVIRONMENTAL RISKS OF NON POINT SOURCE HEAVY METAL CONTAMINATION USING DAIS SENSOR

János Tamás[1], Péter Kardeván[2], Elemér Kovács[1], Elza Kovács[1] and Péter Takács[1]

1. University of Debrecen, Department of Water and Environmental Management, Hungary; e-mail: tamas@gisserver1.date.hu; elkovacs@gisserver1.date.hu; ekovacs@gisserver1.date.hu; ptakacs@gisserver1.date.hu
2. Geological Institute of Hungary e-mail: kardevan@euroweb.hu

ABSTRACT

Abandoned mining sites cause environmental problems all over the world, in Europe as well. The point source heavy-metal contamination, which later becomes diffuse pollution endangers the environment in the long term. With the use of hyperspectral remote sensing the spatial distribution of certain contaminants can be determined. Due to the acidification of the environment caused by the pyritic decay/ weathering of the tailings, the mobilization and migration of heavy-metals can be observed. Remote sensing techniques can be used effectively for the simultaneous investigation of these processes.

The abandoned mining site of Gyongyosoroszi covers about 28 hectares with approximately 3 million tons of heavy-metal rich mining waste without proper precautions for the protection of the surrounding area. On the predominantly uncovered slopes of 15-20% the occasional high intensity precipitations pose significant environmental risk.

The hyperspectral data file - obtained by the DLR 2002 HySens hyperspectral flight campaign – was analyzed for sphalerite, galenite and its derivatives - minerals typical at mining sites. The results are used for the validation of USLE (Universal Soil Loss Equation) model, which allows the more reliable assessment of environmental risks and planning of site remediation and phytostabilization of the contamination. The DLR DAIS sensor recorded spectra at SWIR I,II (1,5-1,8; 2,0-2,5), which was used for the determination of heavy-metal containing minerals, and the spectrum of VIS/NIR (0,43-1,05) was used for providing information on net vegetation production of the area. Parallel to the flight campaign an intensive field survey/investigation was carried out which included DGPS georeferenced positioning, (Trimble) and on-site determination of heavy-metal content of the tailings by a field portable X-ray fluorescence device (NITON XL-703).

The C-factor (crop) of the USLE erosion model was derived from the remote sensing data which ensure the real time upgrading of the land cover.

INTRODUCTION

Soil contamination by heavy metals derived from mining wastes pose serious threat to the terrestrial and aquatic environment and humans. Mining activities affect relatively small areas, but can have a large local impact on the environment (i). Release of metals from mining sites occurs primarily through acid mine drainage and erosion of waste dumps and tailings deposits (ii, iii).

Waste dumping grounds containing elevated concentrations of heavy metals can be a continuous source of metals spreading to the surroundings (iv, v).

Based on a digital elevation model (DEM), the directions of potential material transport resulting from water erosion can be identified for a mine tailing, and the runoff and erosion rates can be estimated by using the Smith-Wischmeier equation (vi, vii). Hyperspectral imagery has been used to detect and map a wide variety of materials having characteristic reflectance spectra for mineral mapping and to detect soil properties including moisture, organic content and salinity (viii). Vegetation scientists have used hyperspectral imagery to identify vegetation species, study plant canopy chemistry and detect vegetation stress.

The modeling of the environmental impacts of mining waste has come into focus, since several potential pollution sources, such as mine tailings, can be found in water catchment areas. The main objective of the field survey was data collection supplemented with remotely sensed data to investigate and evaluate the potential erosion risk of an abandoned mining site.

The investigation is mainly focused on finding connection between hyperspectral data and the geo-chemical, geo-hydrological processes and vegetation features of the surface.

METHODS

As Jordan and D'Alessandro (ix) reported the base metal deposit of Gyongyosoroszi in the Matra Mts., Hungary has a 3x4 km^2 horizontal and about 400 m vertical extension with 1,3 % Pb and 3.5% Zn content. The dams containing the flotation waste burst many times and the mud with 5% sulphide mineral content entered the valley and the Toka-stream. The total tailings loss amounted to approximately 800 tons of galenite (PbS) – sphalerite (ZnS) concentrates. The maximum heavy-metal concentrations are found in the "yellow sand" (oxidized tailings) deposited on the narrow floodplain of the stream. Escaped tailings mud was carried by stream water and more than 100,000 m^3 of contaminated mud was deposited in downstream industrial and agricultural water reservoirs. Flotation mud took 1/3 of reservoir capacity of a downstream agricultural reservoir that has to release water through a bottom release in flood events. Thus contaminated mud is released from the reservoir as a secondary pollution source long after mine closure.

Field surveying methods

Mátra mountains: soil, water and stream bed samples for mine-originated contamination analysis by ITC, JRC and MAFI and University of Debrecen. 50 soil samples were analysed in ITC for heavy metal content. Field and laboratory spectra were taken from the same samples to establish correlation between the samples and the images. The JRC Hysens Team collected 640 soil samples from the top of waste rock dumps and tailings heaps in Gyongyosoroszi mining area. Vegetation (reed) samples were taken and analysed for contamination-induced stress from the mine waste dumps. Soil samples were prepared for subsequent laboratory analysis. Soil sampling and spectral measurement sites by JRC and MAFI were represented in GIS layers, field data have been pre-processed, digital photos and field spectra, spectral profiles, site polygons sampling points are available. A spectral library was compiled as well by JRC team. Distribution of contaminants was evaluated by geo-statistical methods with Surfer 8 software, and taken into consideration for the calculation of the heavy metal load to the environment of the mine tailing. In situ analysis was applied, and total heavy metal concentrations were measured, including Mo, Zr, Sr, Rb, Pb, Se, As, Hg, Zn, Ni, Co, Fe, Mn and Cr, with a NITON XL 700 field portable X-ray fluorescent spectrometer. Data processing was done using Surfer 8, ArcGIS and Grapher 3 software.

The hyperspectral sensor

In the frame of the first hyperspectral flight campaign in Hungary the Digital Airborne Imaging Spectrometer DAIS 7915 was used. The device is a 79 channel high resolution optical spectrometer which collects information from the Earth's surface in the 0.4 - 12.6 µm wavelengths region while scanning from an aircraft, electronically processes this data into digital format consisting of 16 bit words, and records these digital data on a cartridge recorder.

Spectral band specifications, main radiometric, and geometric instrument parameters of the DAIS 7915 (Digital Airborne Imaging Spectrometer).

79 spectral/wavelength bands from visible to infrared radiance

450-2450 nm: 72 narrow bands enables the investigation of procedures/processes on the surface with special regard to the vegetation-soil system

8000 - 12000 nm: 8 bands provide data on temperature conditions as well as on the radiance of surface objects

The resolution of the images vary according to the flight altitude of the plane carrying the spectrometer; pixel size is usually between 3-20 meter

Six spectral channels in the 8000 - 12000 nm region could be used for the retrieval of temperature and emissivity of land surface objects. These and 72 narrow band channels in the atmospheric windows between 450 and 2450 nm allow to investigate land surface processes with a special emphasis on vegetation / soil interactions.

Wavelength range: 400nm - 12.6µm, 4 Spectrometers, 79 bands

400 - 1000 nm : 32 Bands, Bandwidth = 15-30 nm Detector: Si

1500 - 1800 nm : 8 Bands, Bandwidth = 45 nm Detector: InSb

2000 - 2500 nm : 32 Bands, Bandwidth = 20 nm Detector: InSb

3000 - 5000 nm : 1 Band , Bandwidth = 2.0 µm Detector: InSb

8000 -12600 nm : 6 Bands, Bandwidth = 0.9 µm Detector: MCT

We used ENVI 4.1 for the analysis. The flight strips are difficult to integrate into a GIS and digitally mosaic due to inherent distortions associated with line-scanner technology. Orthophotographs are recommended as the base for the GIS. Portions of the flight strips can be digitally warped to the orthophotographs over key areas of interest (*Figure 1*).

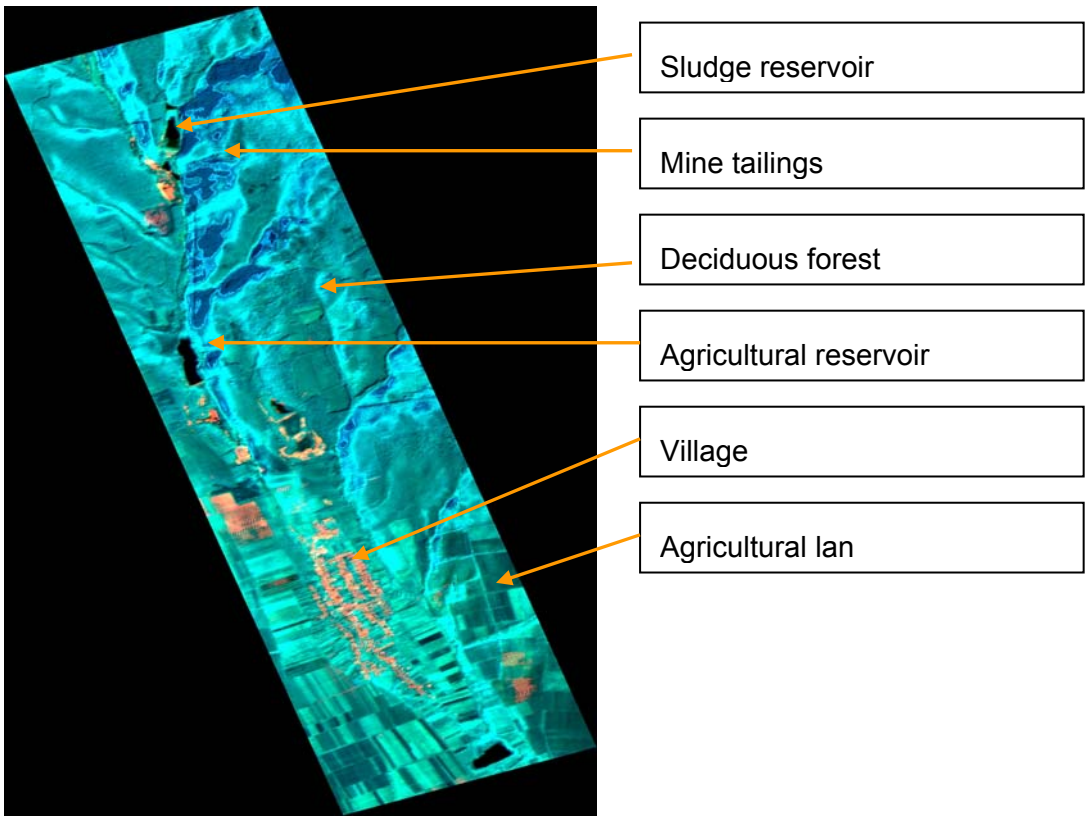

Figure 1: Hyperspectral image of the research area

Calibration

Calibration of a remote sensing sensor is the procedure to establish the conversion parameter that translates output of the sensor to a measurable physical unit.

Atmospheric correction was carried out using the GER 3700 Field Portable Spectroradiometer. The calibration data are used for the systematic correction of the hyperspectral imaging spectrometer data obtained during its in-flight data registration.

By the advanced analysis of the spectral data we performed the measurement of noise characteristics of the sensor channels. The atmospheric correction is based on the MODTRAN radiative transfer code. Image data in the reflective channels of the DAIS sensor are converted to ground reflectance. From the thermal channels emissivities and surface temperatures are derived. Special features include the calculation of water leaving radiance, radiation fluxes and heat fluxes. To assess the stability of the sensor calibration, an interactive software was used for carrying out an in-flight calibration based on measurements of selected ground targets and observed atmospheric data.

The orthophotographs and LANDSAT TM images of the mining site were also used for the analysis and a digital elevation model (DEM) with a vertical accuracy of 1 m was developed.

Landsat TM

Landsat TM provides relatively good spectral resolution with its seven sensors or "bands". These bands measure light reflectance at distinct locations along the electromagnetic (light) spectrum: visible blue (.45-.52 micrometers or μm), visible green (.52-.60μm), visible red (.63-.69μm), near infrared (.76-.90μm), mid-infrared (1.55-1.75μm), mid-infrared (2.08-2.35μm), and far infrared (10.4-12.5μm).

RESULTS

A digital spatial water erosion model was generated in a Geo Information environment for the site, where nearly 7 Mm3 of heavy metal (Pb, Zn, Cd, Cu, Ni, As) rich mining waste was abandoned in 1989. The mine waste is partly under water, lakes are located on three stages of the tailing, and to some extent, the tailing is covered with inert coarse material and vegetation, except the slopes. As a result, the fine mining waste can easily be eroded, contaminating the surrounding areas.

The input data for the estimation of runoff directions of the tailing material include the basic spatial parameters, in high resolution. The potential runoff directions and the area considered to be a source of heavy metal load to the environment were evaluated using a DEM and a digital orthophotograph. The generated grid-based digital elevation model of the site proves that basically the southern and the western part of the tailing are subjected to water erosion, and the former can affect the surroundings to a higher extent, including a stream (Figure 2).

Data collection was carried out using a GPS and the DEM was generated in GIS environment.

The area subjected to erosion in the south was calculated from the data (x, y and z, in meter) given in the unified Hungarian projection system (EOV) with interpolation, and equals approximately 23,000 m^2.

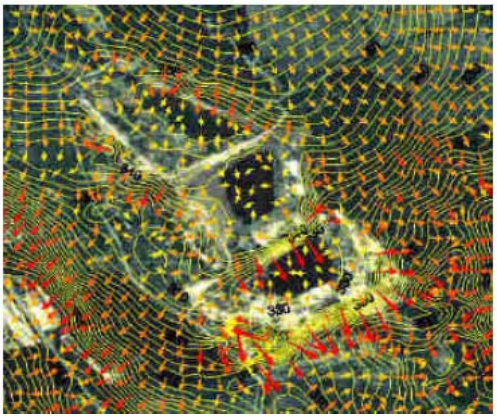

Figure 2: Runoff directions of the mine tailings

To calculate the extent of erosion and the annual medium loss for the area considered a contamination source, based on the DEM, the Smith-Wischmeier equation was used:

E = R K L S C P

where E is the mean annual soil (medium) loss in t ha-1 y-1, R is the rainfall erosivity factor, K is the soil erodibility factor, L is the slope length factor, S is the slope steepness factor, C is the crop management factor and P is the erosion control practice factor. K, L, S, C, and P are dimensionless factors.

The annual medium loss was estimated by characterizing the southern slope with the factors involved in the Smith-Wischmeier equation. The rainfall erosivity factor (*R*) is 0.65 times higher than the calculated erosion index (*EI*), which is 225 t ha-1 év-1 for the studied area, thus *R* = 146.25 t ha-1 y-1. The soil erodibility factor (*K*) was estimated on the base of soil nomograms. The average content of particles (N = 34) with a size less than 100 μm is 5.82%, while that of particles between 100 μm and 2 mm is 53.12%. The low small particle content obviously results from the grinding technology applied during the ore processing. The humus content is 0-0.2%, the eroded mine tailing material has limited organic matter content, and this only in the case where there is vegetation cover. The structure was considered as moderately grained, and the hydraulic conductivity (*k*) was characterized as moderately high (the magnitude of *k* is 10^{-5} m s-1). As a result, *K* = 0.05. The product of the slope length factor (*L*) and the slope steepness factor (*S*) were calculated on the basis of the average *L* and *S* (*N = 22*), where the slope is 31,28 %, equals 11.93 (*Table 1*).

Table 1: Statistical data used for the estimation of annual medium loss at the eroded site.

	particle size, % <100 μm	particle size, % 100 μm - 2 mm	angle, degree	slope, m
Mean	5.82	53.12	28.16	39.02
Standard error	0.89	2.65	1.93	2.59
Median	4.93	53.42	32.31	44.14
Variation coefficient	3.20	9.57	9.04	12.15
Number of values	34	34	22	22

The crop management factor (*C*) was considered as a weighted sum of factors assigned to different, widely occurring species. Altogether, 39.4% of the slope is covered with vegetation and the remaining 60.6% of the site is uncovered, where *C* = 1. Approximately, 9.8% is covered with *Robinia pseudoacacia*, where *C* = 0.40 as characteristic for degraded deciduous forest, and 29.6% with mainly *Rubus caesious* and other species having poor soil protecting effect, thus *C* is considered 0.6. As a result, *C*, calculated with the help of the data gained from the EOV after digitization of the parts of the area covered with vegetation and on site survey, equals 0.72.

Detailed analysis of the crop management factor can be carried out based on the remote sensing data. NDVI is one of the most common vegetation indices derived from remote sensing observations (x, xi). Economical use of the derived NDVI includes agricultural applications, namely, yield estimation and forecast (xii, xiii).Values of this index are calculated from the reflected solar radiation in the near-infrared (NIR) and red (R) wavelength bands, 580-680 nm, and 730-1100 nm, respectively. NDVI can be determined using the following formula:

$$NDVI=(NIR-R)/(NIR+R).$$

We found that the area with NDVI values lower than 0,19 are mainly the uncovered slopes of the mine tailings, whereas the surrounding forests are represented with an NDVI value above 0,79 (*Figure 3*).

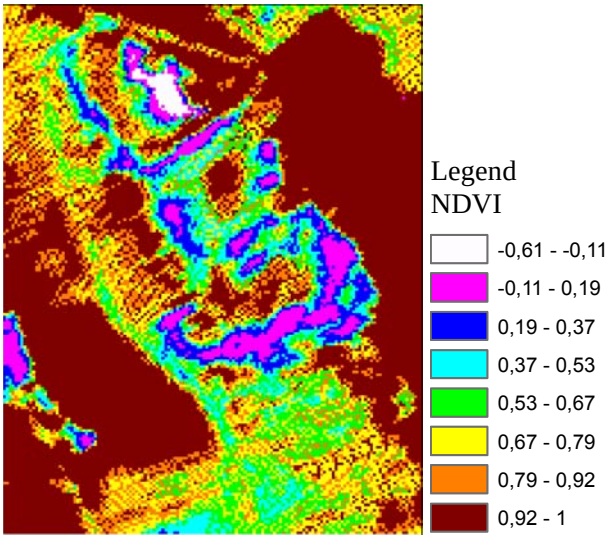

Figure 3: Normalized Vegetation Index image based on DAIS hyperspectral image

The erosion control practice factor (*P*) is considered 1, as the slope is over 30% and there is not any agro-technical practice applied at the site.

The overall heavy metal release resulting from erosion at the south slope of the mine tailing was calculated from the annual medium loss and the characterizing heavy metal concentrations, including those of lead, arsenic, zinc and iron (*Table 2*).

Table 2: Statistical data of the heavy metal concentrations (mg kg-1) measured at the eroded site

	Pb	As	Zn	Fe
Mean	592,63	122,44	3269,32	44564,27
Standard error	77,184	5,497	982,098	1717,603
Median	181,2	83	267,8	38784
Variation coefficient	2,856	0,894	6,635	0,856
Number of values	481	397	488	494

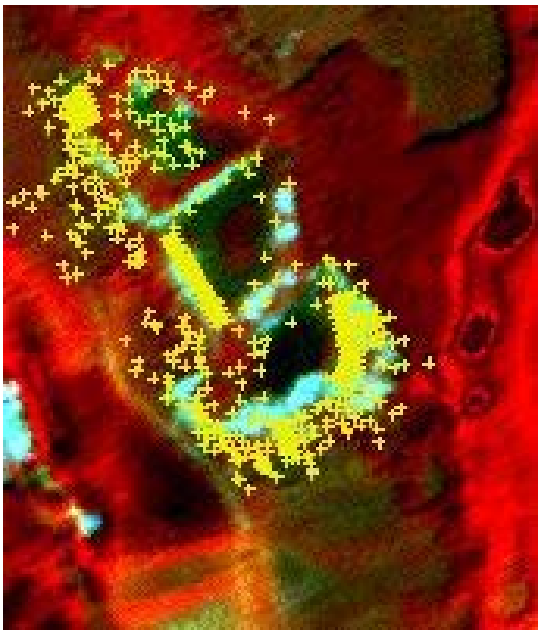

Figure 4: Hyperspectral image of the mining site. Yellow crosses indicate the sampling points for heavy metal analysis.

As a result, the annual medium loss (*E*) equals 62.81 t ha-1 y-1 , which represents 144.47 t y-1 for the studied slope area. Taking the heavy metal concentrations into account, the heavy metal load to the surroundings of the tailing resulting from erosion equals 26.22 kg y-1 for lead, 14.99 kg y-1 for arsenic, 42.19 kg y-1 for zinc and 658.03 kg y-1 for iron (*Figure 4*).

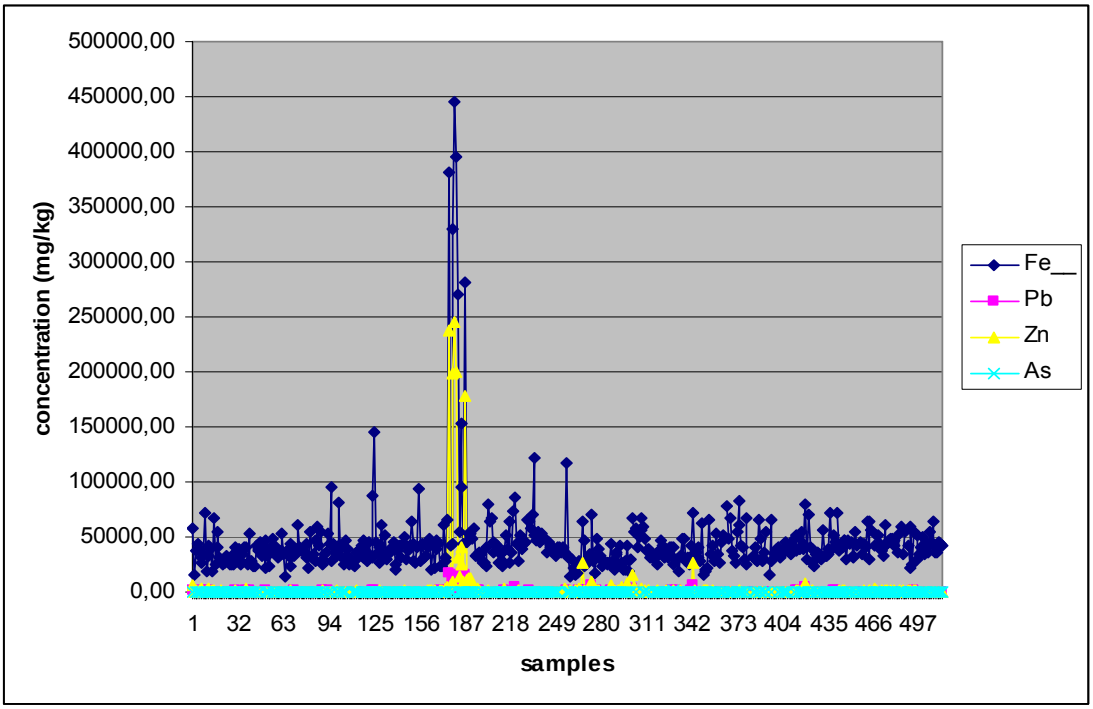

Figure 5: Heavy metal content of soil samples

The correlation coefficient between the different metal content of the samples were calculated. The highest correlation was found between Pb and Zn (r=0,9), Fe and Zn (r=0,88) and between Fe and Pb (r=0,83). The correlation between Fe and As; Zn and As; and between Pb and As content of the samples was found much lower: r = 0,37; 0,22 and 0,41 respectively (*Figure 5*).

The mining of volcanogenic sulphide ore deposits resulted in the exposure of sulphide bearing rocks to surface water and atmospheric oxygen, which accelerate oxidation, leaching and release of metals, a process called Acid Mine Drainage (AMD). Pyrite exposed at the surface of these tailings readily oxidizes to form hematite, goethite or jarosite.

With the use of hyperspectral imagery we attempted to map the distribution of pyritic minerals e.g. jarosite (KFe3(SO4)2(OH)6) and goethite (FeO(OH)) in the area. The jarosite contribute substantially to the acidification process and thereby the mobilization of heavy metals. We performed the spatial analysis of sphalerite ((Zn, Fe)S) and galenite (PbS) as well as the buffering minerals e.g. calcite and illite.

Common rock-forming minerals exhibit wavelength dependent spectral features throughout the VNIR (0.4–1.0 Am), SWIR (1.0–2.5 Am), and TIR (5–25 Am) wavelength ranges. In the 8- to 12-Am TIR atmospheric window region, mineral groups such as silicates, carbonates, sulfates, and phosphates have spectral features related to the fundamental vibrational frequencies of their interatomic bonds. The identification of sulfate salts with hyperspectral imagery has significant implications for remote sensing applications in regional monitoring of acid rock drainage potential.

CONCLUSIONS

Based on the processing of hyperspectral data we found that hyperspectral imagery can be effectively used for the assessment of environmental conditions of large areas. In order to acquire more reliable data and better accuracy, field or laboratory measurements has to be performed for the

validation of hyperspectral data. In case of geological/mineral surveying the effect of vegetation cover has to be taken into account.

The digital elevation model of the studied mine tailing and other data sources provide useful information on the potential of the erosion processes. Combined with the maps of heavy metal concentration distribution, particle size distribution and vegetation, the environmental risk and magnitude of erosion can be calculated. As a result, the environmental impact of the mining waste can be analyzed and a cost-effective treatment, which is also environmentally adequate, can be suggested and performed. In Gyöngyösoroszi, the mine tailing has an impact on its surroundings only on its southern part. However, here the erosion rate is considerable and a stream may also be affected, resulting in potential surface water contamination.

The annual medium loss (*E*) calculated from mean values characterizing the slope subjected to erosion to the highest extent on the mine tailing equals 144.47 t y-1. The heavy metal load, to the surroundings of the tailing resulting from erosion, equals 26.22 kg y-1 for lead, 14.99 kg y-1 for arsenic, 42.19 kg y-1 for zinc and 658.03 kg y-1 for iron.

The values given above are the results of estimates made without a large amount of measured data and specific erosion modeling software, especially for the calculation of the factors of the soil loss equation. However, the geo- information system, including the digital elevation model and the orthophotograph of the site, provided a strong basis for analyzing the magnitude – and in this way, the risk – of the heavy metal load.

References

i. Salomons, W.: 1995. Environmental impact of metals derived from mining activities: processes, predictions, prevention. Journal of Geochemical Exploration, 52(1-2), 5-23.

ii. Yan, G., Bradshaw, A.D.: 1995. The containment of toxic wastes: II. Metal movement in leachate and drainage at Parc Lead-Zinc Mine, North Wales, Environmental Pollution, 90(3), 379-382.

iii. Szücs A., Jordán Gy., Qvarfort, U.: 2000. Integrated modelling of acid mine drainage impact on a wetland stream using landscape geochemistry, GIS technology and statistical methods. In: Fabbri, A. (ed.), Deposit and Geo-environmental Models for Resource Exploitation and Environmental Security. NATO ASI Series Book. Kluwer Academic Publishers.

iv. Vangronsveld, J., Sterckx, J., Van Assche, F., Clijsters, H.: 1995. Rehabilitation studies on an old non-ferrous waste dumping ground: effect of revegetation and metal immobilization by beringite. Journal of Geochemical Exploration, 52, 221-229.

v. Dudka, S., Adriano, D.C.: 1997. Environmental impacts of metal ore mining and processing: A review. Journal of Environmental Quality, 26, 590-602.

vi. Wischmeier, W.H., Smith D.D.: 1978. Predicting rainfall erosion losses. USDA Agricultural Research Service Handbook 537.

vii. Morgan, R.P.C.: 1995. Soil Erosion & Conservation. 2nd Ed. Longman.63-83.

viii. Ben-Dor, E.: 2002. Quantitative remote sensing of soil properties. Advances in Agronomy, Vol. 75, 173-243.

ix. Jordan, G., D'Alessandro, M.: (2004) Mining, mining waste and related environmental issues.: problems and solutions in Central and Eastern European Candidate Countries, Office for Official Publications of the European Communities, pp. 21-21

x. Justice, C.O., Townshend, J.R.G., Holben, B.N., Tucker, C.J., 1985. Analysis of the phenology of global vegetation using meteorological satellite data. International Journal of Remote Sensing 8, 1271–1318.

xi. Townsend, J., Justice, C., Li, W., Gurney, C., McManus, J., 1991. Global land cover classification by remote sensing: present capabilities and future possibilities. Remote Sensing of Environment 35, 243–255.

xii. Hamar, D., Ferencz, C., Lichtenberger, J., Tarcsai, G., Ferencz-Arkos, I., 1996. Yield estimation for corn and wheat in the Hungarian Great Plain using Landsat MSS data International Journal of Remote Sensing 17, 1689–1699.

xiii. Rasmussen, M.S., 1997. Operational yield forecast using AVHRR NDVI data: reduction of environmental and inter-annual variability. International Journal of Remote Sensing 18, 1059–1077.